Deciphering the DSB repair mechanisms involved in CRISPR-induced mutagenesis and gene targeting in the model plant, *Physcomitrella patens*.

Cécile Collonnier[1,*], François Maclot[2], Aline Epert[1], Kostlend Mara[1], Anouchka Guyon-Debast[1], Florence Charlot[1], Fabien Nogué[1].

[1] INRA Centre de Versailles-Grignon, IJPB (UMR1318) - route de St-Cyr, F-78026 Versailles cedex, France.

[2] Gembloux Agro-Bio Tech, Université de Liège, Unité de Biologie végétale - 2 Passage des Déportés, B-5030 Gembloux, Belgique.

Scientific context

Site-directed nucleases are very efficient tools to mutate defined genomic sequences (knock-out) and to direct the insertion of a template DNA at a specific target (knock-in). The DNA repair mechanisms that are presumed to be mainly involved in these two types of events are respectively canonical non-homologous end-joining (c-NHEJ) and, if the template shares homology to the target, homologous recombination (HR). By using, the model plant *Physcomitrella patens,* where efficient gene editing (knock-out or knock-in) via SDN can be obtained, we demonstrated that it may not be as simple.

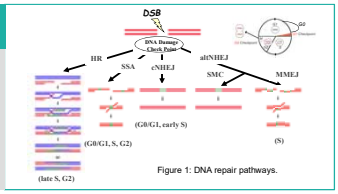

Figure 1: DNA repair pathways.

Materials and Methods

We tested a wild type strain of *P. patens* (Ashton & Cove, 1977) and several mutants produced in the lab: *ΔΔ Pp rad51-1-2* and *Δ Pp rad51b* impacted in HR, *Δ Pp rad1* and *ΔΔ Pp rad1-10* impacted in Single Strand Annealing (SSA) and potentially Microhomology-Mediated End Joining (MMEJ), *Δ Pp lig4* impacted in c-NHEJ, and *Δ Pp mre11* involved in the DNA damage checkpoint.

Two sgRNAs matching respectively two target loci in exon 3 (sgRNA#2) and exon 5 (sgRNA#1) of the *PpAPT* reporter gene were designed and cloned into expression vectors under the control of a *P. patens* U6 promoter. The Cas9 nuclease we used was an Arabidopsis codon-optimized version of the Cas9 protein from *Streptococcus pyogenes* placed under the control of the rice Actin 1 promoter (McElroy *et al*., 1990).

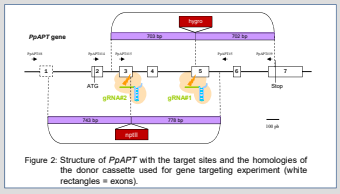

Figure 2: Structure of *PpAPT* with the target sites and the homologies of the donor cassette used for gene targeting experiment (white rectangles = exons).

P. patens protoplasts were transformed by PEG fusion and free-living plants were regenerated (Schaefer et al., 1997).

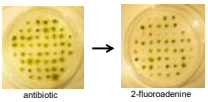

Figure 3: *P. patens* clones subcultured on selective media after transformation using the CRISPR/Cas9 system.

To study CRISPR-induced mutagenesis, one plasmid bearing the Cas9 and the sgRNAs targeting the *PpAPT* reporter gene was used. Mutated clones were selected by cultivating the regenerating protoplasts on a medium containing 2-fluoroadenine (2-FA), a molecule allowing the survival only of cells with a non-functional *PpAPT* gene. The mutation rates were estimated by dividing the number of resistant plants on 2-FA by the number of growing colonies after 5 days on regeneration medium. These mutations were sequenced using primers surrounding the targeted loci.

To evaluate the frequency of gene targeting, protoplast were co-transformed with a plasmid bearing a "Cas9 + sgRNA" construct and a plasmid bearing a knock-out cassette with an antibiotic resistance gene surrounded by *PpAPT* gene sequences flanking the target (Fig. 2). Regenerating moss clones were sequentially sub-cultured on media containing first the antibiotic corresponding to the knock-out cassette used and then 2-FA (Fig.3). Their target sites were then genotyped to identify the nature of the insertions (Fig.4).

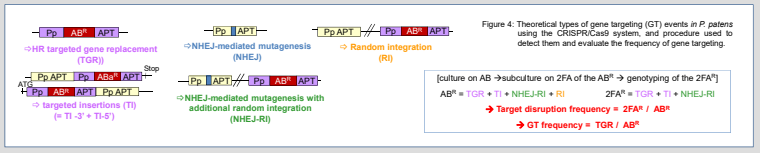

Figure 4: Theoretical types of gene targeting (GT) events *in P. patens* using the CRISPR/Cas9 system, and procedure used to detect them and evaluate the frequency of gene targeting.

Results

CRISPR-induced mutagenesis (no template DNA)

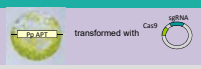

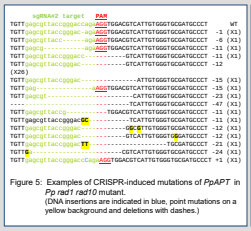

Figure 5: Examples of CRISPR-induced mutations of *PpAPT* in *Pp rad1 rad10* mutant.
(DNA insertions are indicated in blue, point mutations on a yellow background and deletions with dashes.)

Table 1: CRISPR-induced mutation frequencies in *P. patens* wild type clone and mutant clones impacted in different DNA repair pathways.

(Nb of regenerant clones = nb of protoplasts in intense division 5 days after the transformation, nb 2FA^R clones = nb of free-living regenerated plants with a mutated target).

	Nb regenerant clones	Nb 2FA^R	Mutation frequency (%)
WT	8250	298	**3,6**
rad51-1/2	22000	840	**3,82**
rad51b	19800	796	**4,0**
rad10	7425	243	**3,3**
rad1-10	17250	536	**3,1**
mre11	88000	4800	**5,45**
lig4	19500	765	**3,92**

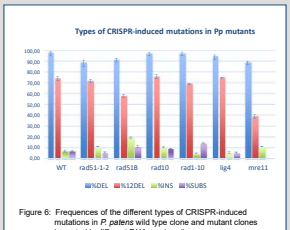

Figure 6: Frequences of the different types of CRISPR-induced mutations in *P. patens* wild type clone and mutant clones impacted in different DNA repair pathways.
(%DEL = % of plants with deletions, %12DEL = % of plants with the very frequent 12bp-deletion potentially due to MMEJ-driven repair of the CRISPR-induced DSB, %INS = % of plants with insertions, % of plants with substitutions).

- As expected, no significant differences in the frequency and the nature of the CRISPR-induced mutations could be observed between PpWT and the mutants potentially impacted in the HR and SSA pathways: *Δ Pp rad51*, *Δ Pp rad51b*, *Δ Pp rad10*, *ΔΔ Pp rad1-rad10*.

- Less « MMEJ-type deletions » (12bp-deletions potentially due to MMEJ-driven repair of the CRISPR-induced DSB) was detected in Δ*mre11*, a mutant impacted in the processing and the resection of DSB ends. However, *Δ Pp mre11* shows the same mutation frequency as the WT. This could mean that the potential reduction in MMEJ-repair is compensated by another mechanism capable of inducing mutagenesis as well.

- No decrease of « MMEJ-type deletions » was observed in *Δ Pp rad10* and *ΔΔ Pp rad1/rad10*, which could either mean that MMEJ is not involved in these 12bp-deletions, or that it is another complex that trims the flapping ends generated in this pathway.

- Surprisingly, no significant differences in the frequency and the nature of the CRISPR-induced mutations were detected in *Δ Pp lig4* !
Could it mean that canonical NHEJ (c-NHEJ) is not involved in CRISPR-induced mutagenesis in *P. patens* ?
Is another type of end-joining using another ligase than LIG4 doing the job ?

CRISPR-induced gene targeting (+ template DNA)

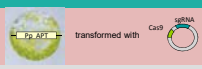

Table 2: CRISPR-induced target disruption frequencies in *P. patens* wild type clone and mutant clones impacted in different DNA repair pathways.

(Relative Transformation Frequencies (RTF) express the frequency of stable AB^R clones in the population of regenerated clones.).

	Nb regenerant clones	Nb AB^R clones	RTF (%)	Nb 2FA^R clones	% target disruption	% GT without CRISPR (linear template)
WT	94800	49	0,516 ± 0.02	49,00	100,00 ± 0	65
rad1	74700	32	0,428 ± 0.05	32,00	**100,00** ± 0	**31.6**
WT	86500	104	1,2 ± 0.09	98	94,23 ± 0.02	65
rad51-1/2	58000	105	1,81 ± 0.11	97	**92,38** ± 0.13	**0**
WT	81525	50	0,613 ± 0.06	50,00	100,00 ± 0	65
rad51b	74475	79	1,06 ± 0.04	78,00	**99,00** ± 0.01	**0**

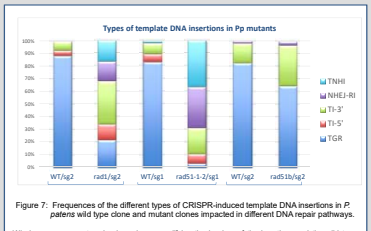

Figure 7: Frequences of the different types of CRISPR-induced template DNA insertions in *P. patens* wild type clone and mutant clones impacted in different DNA repair pathways.

(All clones were genotyped using primers amplifying the borders of the insertions and the wild type sequence of the target : TGR clones presented both borders and no WT band; TI-5' and TI-3' presented the WT band and respectively the 5' border or the 3' border; NHEJ-RI presented the WT band with a mutation but no borders, **TNHI** presented no borders but no WT band either, which could indicate **a targeted insertion of the donor DNA but not based on the homologies of the template DNA**).

- Surprisingly, no significant differences in the frequencies of target disruption were observed between WT and the mutants Δ *Pp rad1*, ΔΔ *Pp rad51-1/2* and Δ *Pp rad51b* impacted in the HR and SSA/MMEJ pathways (Tab. 2).

- In WT, the CRISPR/Cas9 system increases the nb of TGR events (~80% (Fig. 7) vs ~50% without CRISPR, data not shown).

There is also always more TI-3' than TI-5' (Fig. 7). This could be due to the fact that CRISPR-induced DSBs often trigger resection upstream the PAM.

- In Δ *Pp rad1*, TI events are not decreased compared to the WT. This could mean that SSA/MMEJ are not the only mechanisms involved in the production of CRISPR-induced TI events. Some other kinds of End-Joining may be involved as well.

- In Δ *Pp rad51-1-2*, GT is decreased compared to WT, and especially TGR events , indicating that **CRISPR-induced GT is RAD51-dependant. BUT NOT ONLY !**
Indeed, there is still some TGR and TI events, meaning that, when HR is not available, there is still **insertion of the circular template DNA based on the homologies of the knock-out cassette** (as the sequencing of the borders of the inserts confirm it).
This could be due to some microhomology-driven repair such as **SSA/MMEJ.**

- In Δ *Pp rad1* and ΔΔ *Pp rad51-1/2*, some **TNHI events** (Targeted Non-Homology driven Insertions, see caption of Fig.7) were also detected indicating that a large DNA fragment had probably been inserted at the target, not by HR (since no borders could be detected) but by illegitimate insertion not based on the homologies present in the template DNA (potentially via **SSA/MMEJ or some other kind of End-Joining**).

Conclusions

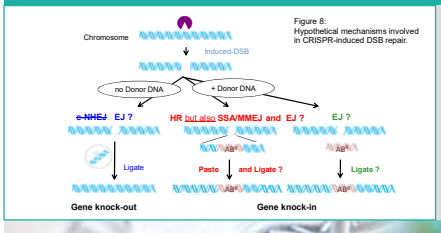

Figure 8:
Hypothetical mechanisms involved in CRISPR-induced DSB repair.

By applying the CRISPR/Cas9 system to a series of mutants impacted in different DNA repair pathways, we progressed in the understanding of the mechanisms that could be involved in CRISPR-induced mutagenesis and gene targeting in plants. Without template DNA, we showed that the mutation efficiency was not decreased in absence of key factors of c-NHEJ, which could indicate that CRISPR-induced mutations may not only be due to c-NHEJ but also to alternative end-joining like micro-homology mediated end joining (MMEJ) and other types of non-canonical end joining. Targeted insertion of a circular template DNA presenting homology to the target appeared to be mainly dependent on the RAD51-dependent HR pathway but not entirely, and other pathways, including single-strand annealing (SSA), could potentially be involved.

*** contact : cecile.collonnier@versailles.inra.fr**

This work was supported by the French programme "Investissements d'Avenir" and by the French National Research Agency through the research project GENIUS | ANR-11-BTBR-0001.